JMolMed

ORIGINAL ARTICLE

A DNA methylation signature associated with the epigenetic repression of glycine *N*-methyltransferase in human hepatocellular carcinoma

Covadonga Huidobro · Estela G. Toraño · Agustín F. Fernández · Rocío G. Urdinguio ·
Ramón M. Rodríguez · Cecilia Ferrero · Pablo Martínez-Camblor · Loreto Boix ·
Jordi Bruix · Juan Luís García-Rodríguez · Marta Varela-Rey · José María Mato ·
María Luz Martínez-Chantar · Mario F. Fraga

Abstract The basic mechanisms underlying promoter DNA hypermethylation in cancer are still largely unknown. It has been proposed that the levels of the methyl donor group in DNA methylation reactions, *S*-adenosylmethionine (SAMe), might be involved. SAMe levels depend on the glycine-*N*-methyltransferase (GNMT), a one-carbon group methyltransferase, which catalyzes the conversion of SAMe to *S*-adenosylhomocysteine in hepatic cells.

Covadonga Huidobro and Estela G. Toraño contributed equally to this work.

C. Huidobro · E. G. Toraño · A. F. Fernández · R. G. Urdinguio ·
R. M. Rodríguez · C. Ferrero · M. F. Fraga (✉)
Cancer Epigenetics Laboratory, Instituto Universitario de Oncología del Principado de Asturias (IUOPA), HUCA, Universidad de Oviedo, 33006 Oviedo, Spain
e-mail: mffraga@cnb.csic.es

P. Martínez-Camblor
Unidad de Apoyo a la Investigación CAIBER, OIB, Oviedo, Spain

L. Boix · J. Bruix
Liver Unit, Barcelona Clinic Liver Cancer (BCLC) group, Hospital Clinic Barcelona, IDIBAPS, University of Barcelona, Spain. Centro de Investigación Biomédica en Red de Enfermedades Hepáticas y Digestivas (CIBERehd), Barcelona, Spain

J. L. García-Rodríguez · M. Varela-Rey · J. M. Mato ·
M. L. Martínez-Chantar
CIC bioGUNE, Centro de Investigación Biomédica en Red de Enfermedades Hepáticas y Digestivas (CIBERehd), Bizkaia, Spain

M. F. Fraga
Department of Immunology and Oncology,
National Center for Biotechnology, CNB-CSIC, Cantoblanco, Madrid 28049, Spain

GNMT has been proposed to display tumor suppressor activity and to be frequently repressed in hepatocellular carcinoma (HCC). In this study, we show that GNMT shows aberrant DNA hypermethylation in some HCC cell lines and primary tumors (20 %). GNMT hypermethylation could contribute to gene repression and its restoration in cell lines displaying hypermethylation-reduced tumor growth in vitro. In agreement, human primary tumors expressing GNMT were of smaller size than tumors showing GNMT hypermethylation. Genome-wide analyses of gene promoter methylation identified 277 genes whose aberrant methylation in HCC was associated with GNMT methylation/expression. The findings in this manuscript indicate that DNA hypermethylation plays an important role in the repression of GNMT in HCC and that loss of GNMT in human HCC could promote the establishment of aberrant DNA methylation patterns at specific gene promoters.

Introduction

Hepatocellular carcinoma (HCC) is a solid tumor with one of the highest incidences worldwide [1]. Remarkably, the incidence of hepatic cancer varies geographically and within ethnic groups. This variation in HCC distribution may be due to differences in exposure to hepatitis viruses and environmental pathogens [2]. HCC has a poor prognosis, leading to death because of liver failure, which may be caused due to cirrhosis and/or to tumor progression. The survival rate of patients diagnosed with HCC is quite low. When detected at an early stage, HCC can be cured by surgical resection, liver transplantation, or ablation. However, most

tumors are diagnosed at an intermediate or advanced evolutionary stage when such treatment options are of limited efficacy [3]. Factors such as viral hepatitis infections, exposure to aflatoxin B1 (mycotoxin), obesity, excessive alcohol intake, and tobacco are important risk factors for HCC development [4]. They contribute to chronic liver inflammation and alter its regenerative properties. Other entities associated are continued liver damage, hemachromatosis [5], diabetes [6], and non-alcoholic steatohepatitis [7]. Furthermore, genetic and epigenetic changes affecting tumor suppressor genes (TSG) and oncogenes are also involved in hepatocarcinogenesis [8]. In particular, a few genes have been repeatedly studied and found to be silenced by promoter hypermethylation in HCC, for example E-cadherin [9], p16(INK4A) [10, 11], and p14 (ARF) [10]. Unfortunately, the precise mechanisms that originate abnormal DNA methylation reactions in HCC development remain unknown.

Glycine-*N*-methyltansferase (GNMT; EC 2.1.1.20), which catalyzes the synthesis of sarcosine (*N*-methylglycine) from glycine, uses *S*-adenosylmethionine (SAMe) as the methyl donor group [12] and contributes most to transmethylation reactions. Thus, GNMT is a key protein in the regulation of one-carbon metabolism by regulation of SAMe levels. In the case of excess SAMe, GNMT activity is significantly increased, but when SAMe concentration lowers, GNMT is inhibited so that it is conserved for vital methylation reactions [13]. Surprisingly, only three human cases of GNMT deficiency have been reported in the literature, but all of them are characterized by chronic liver disease [14, 15]. Interestingly, it has been described that GNMT experiences mRNA decreases in human HCC in comparison with healthy liver [16, 17]. Moreover, GNMT KO mice develop steatosis, fibrosis, and HCC in a spontaneous way. The loss of GNMT induces aberrant methylation of DNA and histones, resulting in epigenetic modulation of critical carcinogenic pathways in this animal model [18].

SAMe and its precursors prevent the development of liver tumors induced by various carcinogens in rats and mice [19–21] but the underlying mechanisms are still a matter of discussion. Taking into account that GNMT activity is modulated in response to SAMe levels in liver cells [22–24], the protective function of SAMe could be mediated to some extent by GNMT and play an important role in the chemopreventive pathway of liver cancer [25]. This was the first proposal to consider GNMT as an anticancer gene. Since then, several reports support the potential of GNMT as a TSG [18, 26]. The present work aims to elucidate the molecular mechanisms involved in the repression of GNMT in HCC and how this methyltransferase exerts its anticancer function.

Material and methods

Human cancer cell lines culture and primary tumor samples

Three human HCC cell lines (Alex, SNU354, SNU368) were obtained from the American Type Culture Collection (Manassas, VA, USA), and another HCC cell line (HuH7) and one human hepatoblastoma cell line (HepG2) were kindly provided by Dr. María Luz Martínez-Chantar (CiC Biogune, Bizkaia, Spain). Cell lines were grown in DMEM (41965, Gibco, Grand Island, NY, USA) supplemented with 10 % FBS (F6178, Sigma, St. Louis, MO, USA), 1 % non-essential amino acids (M7145, Sigma), and 2 % penicillin/streptomycin (15070, Gibco) at 37 °C in a humidified 5 % CO_2 incubator.

We obtained DNA and RNA from 35 HCCs (for clinicopathological features, see Electronic supplementary material (ESM) Table S1) from the BCLC tissue collection (Hospital Clinic, Barcelona, Spain) and adjacent nontumor liver tissues were analyzed when available. Also, two healthy liver tissues from the Institute of Oncology of Asturias Tumour Bank were included in the study. Informed consent was obtained from all patients included in this study, in accordance with the ethical principles embodied in the Declaration of Helsinki.

Cell culture treatments

Cells were treated with the demethylating agent 5-aza-2'-deoxycytidine (AdC; A3656, Sigma) for 72 h at various concentrations (2.5 and 5 μmol/l). Treatment was refreshed every 24 h.

DNA extraction and promoter methylation analysis

Genomic DNA isolation was performed according to a standard phenol/chloroform/isoamyl alcohol extraction protocol, after a proteinase K digestion. DNA (500 ng) was bisulfite converted with the EZ DNA Methylation Kit (D5006, Zymo Research, Orange, CA, USA) following manufacturer's advice.

Bisulfite pyrosequencing

After PCR amplification of the region of interest using specific primers, we performed bisulfite pyrosequencing with the PyroMark Q24 reagents, equipment and software (Qiagen Iberia S.L., Madrid, Spain) and the Vacuum Prep Tool (Biotage, Uppsala, Sweden), following manufacturers' instructions. The PyroMark Assay Design tool (v. 2.0.01.15) was used to obtain pyrosequencing oligonucleotides, shown in ESM Table S2.

We also used pyrosequencing to determine the methylation status of *LINE1*, a repetitive DNA sequence interspersed among mammalian genes, which correlates with the cellular

methylated cytosines (mC) level in tissues, since DNA repetitive sequences constitute a substantial portion of the human genome [27].

Methylation-specific PCR

In order to focus on interesting regions of GNMT promoter, methylation-specific PCR (MSP) amplification of bisulfite-converted DNA was performed using a set of primers for GNMT, designed with Methyl Primer Express software (Applied Biosystems, Foster City, CA) and listed in ESM Table S2. The positive control for the methylated reaction was in vitro-methylated DNA obtained by methylation of genomic DNA with the CpG Methyltransferase (M.SssI, M0226, New England Biolabs® Inc., Ipswich, MA, USA). PCR products were visualized in Sybr Safe (S33102, Invitrogen, Carlsbad, CA, USA)-stained 2 % agarose electrophoresis gels and observed under UV light.

mRNA extraction and protein analysis by quantitative reverse-transcription

Trizol reagent (15596-018, Invitrogen) was used to extract total RNA from both biopsies and cell lines, according to the manufacturer's instructions. cDNA was synthesized from total RNA (1 μg) using the SuperScript II Reverse Transcriptase Kit (18064, Invitrogen), following the manufacturer's recommendations. The quantitative RT-PCR reaction was performed by mixing the converted cDNA, previously diluted, with Sybr Green 2× Master Mix (4309155, Applied Biosystems) and the primers listed in ESM Table S2. qRT-PCR was carried out on an HT7300 Real-Time PCR System (Applied Biosystems). GAPDH was again used as housekeeping gene to standardize data, following the $\Delta\Delta Ct$ method [28]. Western blot analysis was performed as described in supplementary information.

Chromatin immunoprecipitation

Chromatin immunoprecipitation (ChIP) experiments were carried out following the described protocol (http://www.millipore.com/userguides/tech1/mcpro407), slightly modified. Samples were sonicated to shear chromatin to an average length of 0.2–0.5 kb. Immunoprecipitation was performed with antibodies against H3K4me3 (pAb-003-050, Diagenode, Liège, Belgium), H3K27me3 (07-449, Upstate, Temecula, CA, USA). H4K20me3 (39180, Active Motif, Rixensart, Belgium), and IgG (46540-1, Abcam, Cambridge, UK) as negative control, and H3 (ab1791, Abcam) as positive control. Phenol/chloroform-purified DNA was precipitated and used in ChIP-qPCR assays for GNMT analysis. Primer sequences for ChIP assays are shown in ESM Table S2. Unbound fractions were analyzed as input controls. Results were obtained as fold enrichment of immunoprecipitated DNA associated with the given histone mark, normalized against a 1/200 dilution of input chromatin.

Cell viability assay

Cell viability was determined as described by Mosmann et al. [29]. Cells (1×10^3 per well) were seeded onto 96-well plates. After attachment of cells, 3-(4,5-dimethyl-2-yl)-2,5-ditetrazolium bromide (MTT) was added to medium (500 μg/ml per well) and incubated for 3 h (37 °C, 5 % CO_2). Cell medium was removed and MTT formazan crystals were dissolved in DMSO (100 μl/well). After gently shaking, absorbance at 595 nm was read with a Power Wave WS automated microtitre plate reader (BioTek, U.S., Winooski, VT, USA). Optical density was directly proportional to cell number up to the maximum density measured. Results are expressed as mean±SD of ten replicates.

Cell proliferation rate

Cell proliferation rate was established by cell counting. Cells were seeded in triplicate in 12-well plates at a concentration of 1×10^4 per well. Cells were collected daily for 5 days and viable cells, as assessed by trypan blue staining, were counted under a microscope in a haemocytometer. Results are expressed as the mean±SD of three independent replicates for each time point.

Histone methylation analysis

H3K4me3 and H3K27me3 were analyzed by Western blot. Firstly, histones were extracted from cell pellets in accordance with the acid histone extraction protocol [30]. Approximately, 15 μg of total histones were loaded into a 15 % sodium dodecyl sulfate page gel, following the previously described protocol for Western blot with the antibodies anti-H3K4me3 and anti-H3K27me3 (the same as used in the ChIP assay).

Absolute quantification of S-Adenosylmethionine

SAMe levels were determined by liquid chromatography/mass spectrometry (LC/MS) as previously described [18] with slight modifications.

Statistical analysis

Continuous data were reported as mean±standard deviation and categorical data as absolute and relative frequencies. Statistical analysis was performed with the SPSS software. Student's t test was used for statistical comparisons. Correlations between GNMT methylation or expression and clinicopathological characteristics were assessed by χ^2 test. A p

value of less than 0.05 was considered to be statistically significant. DNA methylation profiling using bead arrays, immunofluorescence assays, and transfection experiments of HuH7 cells were performed as described in ESM.

Results

Hepatocellular carcinoma shows aberrant GNMT DNA hypermethylation

To study the possibility of an abnormal epigenetic regulation of GNMT in liver cancer, we used bisulfite pyrosequencing to determine the methylation status of a region surrounding the GNMT transcription start site (TSS) in healthy liver and in five liver cancer lines (HepG2, SNU368, HuH7, Alex, and SNU354). Using this approach, we identified a region containing seven CpG sites which was unmethylated in nontumorigenic hepatic tissues but densely or moderately methylated in three of the five HCC cell lines (HuH7, Alex, and SNU354) (Fig. 1a, upper panel). These data were further confirmed with MSP (Fig. 1a, lower panel) and 27K Ilumina methylation arrays (ESM Fig. S1).

In order to establish whether the 3′ region of the TSS of GNMT aberrant hypermethylation was also present in vivo, we examined the content of mC by bisulfite pyrosequencing in 35 HCCs. Data obtained revealed that GNMT was hypermethylated in seven out of the 35 primary tumors (20 %; Fig. 1b, upper panel). MSP and bisulfite pyrosequencing confirmed previous data (Fig. 1b, lower

Fig. 1 3′ Region of the TSS of *GNMT* shows aberrant hypermethylation in HCC. To determine the methylation status of the 3′ region of the TSS of *GNMT*, we utilized bisulfite pyrosequencing and methylation-specific PCR (MSP). **a** Diagram representing *GNMT* promoter region in the *upper panel*. The location of each CpG site is represented by *vertical lines* and the *right-angled arrow* indicates the TSS. The Illumina (see ESM Fig. S1) and MSP CpG site analyzed is 273 bp downstream of the TSS, highlighted by a *gray box*. Location of the set of bisulfite pyrosequencing oligonucleotides is indicated by *arrows*. Below, bisulfite pyrosequencing in several hepatic cancer cell lines: HepG2, SNU368, HuH7, Alex, and SNU354. *Bars* indicate target CpG sites and *black* areas represent the percentage of methylated cytosines (mCpG) from 0 to 100, and the

percentage of average methylation is shown on the *left. Lower panel* shows MSP in the cell lines mentioned above. A PCR band under "u" or "m" denotes unmethylated or methylated sequence, respectively. **b** Analysis of the methylation status of the +273 bp CpG site in *GNMT* 3′ region TSS by MSP in 35 primary HCCs in the upper panel. Pie chart shows the percentage of methylated tumors in *black*. Below, MSP reaction of two representative tumors, one methylated and the other unmethylated. Water was used as negative control and IVD (in vitro-methylated DNA) as positive control. In the *lower panel*, bisulfite pyrosequencing of four representative tumors: *U1* and *U2* unmethylated tumors 1 and 2, respectively; and *M1* and *M2* methylated tumors 1 and 2, respectively

panel). These data suggest that aberrant methylation of the 3′ region of the TSS of the *GNMT* gene is also observed in vivo. The region under study belongs to a CpG island located within the TSS of *GNMT*. After determining, by bisulfite pyrosequencing, the methylation rate in different fragments along the CpG island, we found that the 3′ region of the TSS showed the greatest changes in the content of methylated cytosines among all the samples considered (ESM Fig. S2A)

Relationship between GNMT hypermethylation and gene repression

To study the role of *GNMT* hypermethylation in gene expression, we used quantitative RT-PCR and western blot analysis to compare GNMT mRNA and protein levels in healthy liver and the unmethylated HepG2 and SNU368 cell lines with the HuH7, Alex, and SNU354 cell lines, which exhibited dense or moderate *GNMT* DNA hypermethylation (Fig. 2a, ESM Fig. S3A). Intriguingly, *GNMT* mRNA levels were substantially downregulated in the tumor samples, in spite of the absence of methylation in the promoter region (ESM Fig. 2B). *GNMT* repression was inversely related to methylation of the 3′ region of the TSS (Fig. 2a, ESM Fig. S2B). Our results agree with the data in the literature showing that GNMT is downregulated in human HCC. HepG2, which was almost completely unmethylated, showed the highest mRNA levels, although in comparison with healthy tissue, they were still extremely low. This could be explained by the nature of HepG2 as a hepatoblastoma
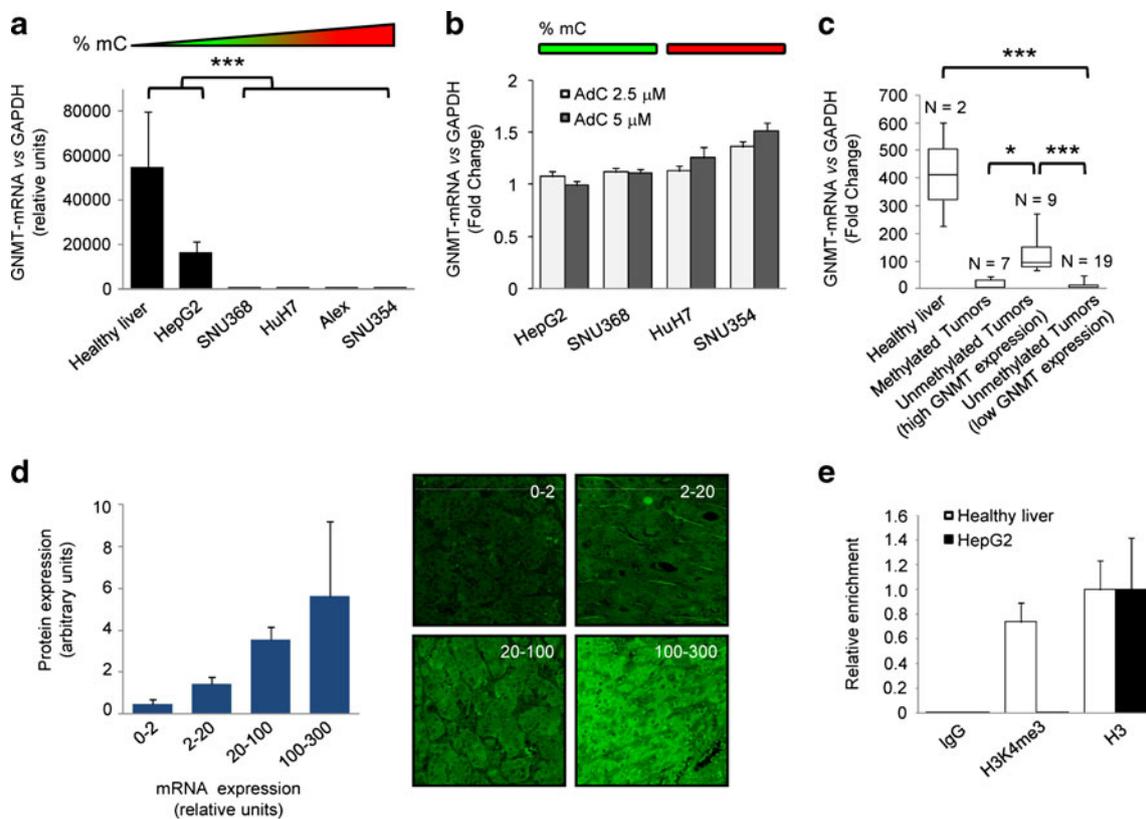
Fig. 2 Expression analysis of *GNMT* in human HCC. **a** Quantitative RT-PCR analysis of GNMT mRNA normalized against GAPDH mRNA in healthy liver and several tumorigenic liver cell lines with different content of mC (*green* hypomethylated, *red* hypermethylated); ***p value<0.001. **b** Effect of the demethylating drug 5-aza-2′-deoxycytidine (AdC) on GNMT mRNA levels. This was evaluated in two hypomethylated cell lines (as indicated by the *green bar* at the *top of the graph*) and two hypermethylated cell lines (*red bar*). Two different concentrations, 2.5 (*gray bar*) and 5 μM (*dark gray bar*), of AdC were tested. For each cell line, GNMT mRNA was normalized against GAPDH mRNA levels and the fold changes were calculated in relation to the untreated cell line (wild type). **c** *Whisker* plots summarizing GNMT mRNA levels in normal tissue and HCC grouped by 3′ region of the TSS of *GNMT* methylation status and mRNA levels. GNMT mRNA was normalized against GAPDH mRNA levels and fold changes were calculated in relation to the value from the unmethylated primary tumor with lowest expression level. *p value<0.05, ***p value<0.001. **d** Immunofluorescence of GNMT protein in HCC samples. *Left panel* shows the correlation between GNMT mRNA and protein levels in the examined samples, grouped by mRNA expression levels (relative units): from 0 to 2, from 2 to 20, from 20 to 100, and from 100 to 300. On the right, representative images of immunofluorescence corresponding to each of the groups considered. Magnification, ×60. **e** ChIP assay in healthy liver (*white bar*) and the tumoral HepG2 cell line (*black bar*). *Bars* indicate relative fold enrichment of GNMT immunoprecipitated with IgG (negative control), H3K4me3 and histone H3 (positive control). Data are normalized against 1/200 dilution of input chromatin and then against H3

cell line while the rest are all derived from HCC. GNMT expression in healthy tissue and HepG2 differed significantly from the rest of the cell lines analyzed (p value<0.001).

To investigate whether the methylation status was exerting a strong influence on *GNMT* expression, some of the cell lines under study were treated with the demethylating agent AdC at different concentrations (Fig. 2b). The selected cell lines for AdC treatments were HepG2 and SNU368, in which the 3′ region of the TSS *GNMT* was demethylated, and another two cell lines, HuH7 and SNU354, which showed higher levels of DNA methylation. In those cell lines with the *GNMT* 3′ region of the TSS aberrantly hypermethylated (HuH7 and SNU354), *GNMT* expression was reactivated with the drug at both 2.5 and 5 μM concentrations. By contrast, in the two unmethylated cell lines (HepG2 and SNU368), AdC did not induce such an effect. Focusing on the heavily methylated cell lines, we found an inverse relation between demethylation at the 3′ region of the TSS and *GNMT* mRNA re-activation after AdC treatment, supporting the role of this region in *GNMT* regulation (ESM Fig. S2C). In particular, SNU354, which exhibited the highest methylation rate along the CpG island, experienced the greatest loss of DNA methylation in the 3′ region of the TSS in comparison with other regions of the CpG island (ESM Fig. S2D). These results suggest that transcriptional silencing of *GNMT* gene is associated with hypermethylation of the 3′ region of the TSS in vitro.

In an attempt to investigate the relationship between 3′ region of the TSS hypermethylation and *GNMT* expression in vivo, we analyzed *GNMT* expression at the mRNA level in two healthy livers, 35 HCCs and adjacent nontumor tissue when available (Fig. 2c and ESM Fig. S4, S5). Samples were grouped according to their nature as healthy tissue or as methylated, or unmethylated, GNMT tumor. Levels of GNMT mRNA were in general higher in nontumor samples although each group differed significantly from the rest (Fig. 2c, p value<0.001). Protein levels of representative samples of all groups were also analyzed (ESM Fig. S3B). Independently of the methylation status, HCCs showed lower *GNMT* mRNA levels than their adjacent nontumor tissues (ESM Fig. S5). We then divided unmethylated HCCs into two groups according to GNMT expression so that one group (N=19) lacked *GNMT* expression even in the absence of methylation and the other group (N=9) expressed *GNMT* mRNA (p value<0.001). To determine the relation between *GNMT* mRNA and protein levels, immunofluorescence with an antibody against GNMT was performed in tissue samples. A significant correlation was found between mRNA levels and the amount of detected protein (global p value=0.001; Fig. 2d), which indicated that DNA methylation plays an important role in regulating the presence of GNMT protein in the cell.

To identify other possible epigenetic mechanisms involved in *GNMT* repression, we carried out ChIP using antibodies against H3K4me3, a histone post-translational modification

associated with gene activation [31] in HepG2 because it is the cell line that exhibits low levels of GNMT mRNA in absence of DNA hypermethylation. Healthy liver was used as reference. Results showed that this histone modification was absent in HepG2 cells while healthy liver exhibited strong enrichment of this histone mark (Fig. 2e). Also, we found a significant enrichment in non-expressing *GNMT* HCC of repressive histone marks such as H3K27me3 and H4K20me3 (ESM Fig. S6). This suggests that, in addition to DNA methylation, histone post-translational modification might have an important role in *GNMT* repression in HCC.

Restoration of GNMT in HCC cell lines decreases cell growth and SAMe levels of liver cancer cells but has little impact on global DNA and histone methylation

To assess the functional role of epigenetic-associated repression of *GNMT* in liver cancer, we generated clones of HuH7 cancer cells stably expressing *GNMT* (pCEP4-GNMT; Fig. 3a). Ectopic GNMT expression was within physiological levels (ESM Fig. 3C). Wild-type HuH7 cells show *GNMT* DNA hypermethylation-dependent gene repression. Restoration of GNMT activity in HuH7 induced a decrease in cell viability (p value<0.001) and proliferation (p value 0.011; Fig. 3b). We performed another stable transfection of GNMT in SNU354 a hepatic cancer cell line which also showed *GNMT* hypermethylation associated with gene repression (ESM Fig. S7A). Functional assays confirmed the previous results and showed a decrease in cell viability and proliferation after restoration of GNMT in this HCC cell line (ESM Fig. S7B). These results are in line with the proposed antitumor role of GNMT [18, 26].

To determine the impact of GNMT function on the amount of SAMe in HuH7 cells, we quantified the levels of SAMe in HuH7 pCEP4 and HuH7 pCEP4-GNMT cells. Restoring GNMT in these cells induced a significant decrease in SAMe levels (Fig. 3c), which agrees with previous research [14, 15]. As GNMT regulates SAMe levels, we hypothesized that the aberrant epigenetic repression of GNMT could affect DNA and histone methylation reactions. To address this issue, we first analyzed global DNA and histone methylation in HuH7 pCEP4 and HuH7 pCEP4-GNMT cells. Ectopic expression of GNMT did not induce any noticeable changes in LINE1 methylation (an indicator of total mC; Fig. 3d) nor in global H3K4me3 and H3K27me3 levels (Fig. 3e).

A genome-wide promoter DNA methylation signature associated with GNMT repression in hepatocellular carcinoma

In mice, lack of GNMT had been previously found to be associated with malignant transformation and aberrant DNA methylation [18]. To study potential site-specific DNA
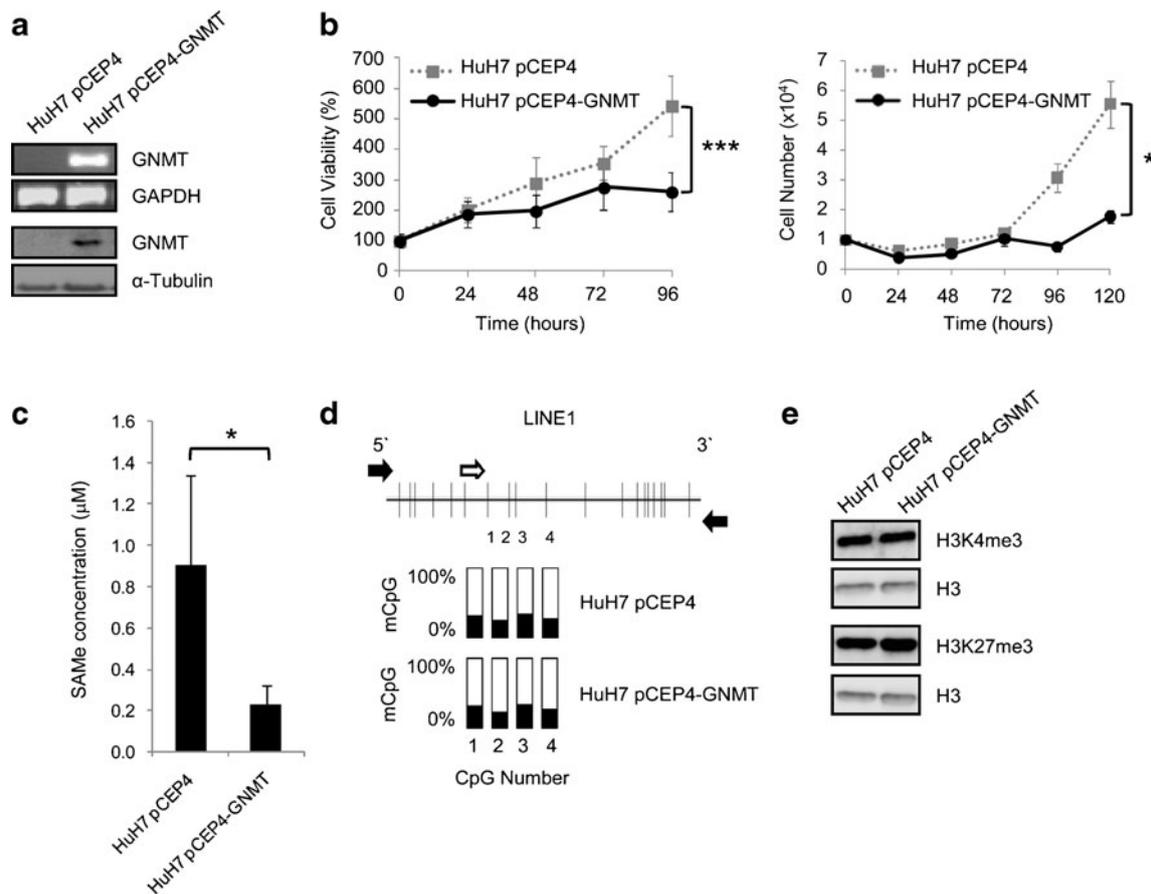
Fig. 3 Restoration of GNMT in the HuH7 cell line and epigenetic and epigenomic consequences. The effects of restoring GNMT were studied in the HuH7 HCC cell line. **a** RT-PCR (*upper panel*) and WB (*lower panel*) of GNMT transfection with the pCEP4-GNMT vector encoding the full-length cDNA of human GNMT sequence and the corresponding empty vector (pCEP4). **b** GNMT overexpression induced a slight decrease in HuH7 cell proliferation and viability. *p value<0.05, ***p value<0.001. **c** Reintroducing GNMT in the HCC HuH7 cell line reduced significantly SAMe concentration (in micromole) (*t test, p value<0.05). **d** Global DNA methylation analysis by bisulfite pyrosequencing of LINE1 in HuH7 after stably transfecting with the GNMT construct (pCEP4-GNMT) and the control vector (pCEP4). *Vertical bars* correspond to the analyzed CpG; *black* highlights methylation (from 0 to 100 %). **e** WB analysis against H3K4me3 and H3K27me3. *Upper panels* show immunoblot of histone marks and *lower panels* correspond to H3 WB, used to normalize data

methylation, alterations associated with the epigenetic repression of *GNMT* in human HCC, we used 27K Illumina methylation arrays to compare the genome-wide promoter methylation status in HuH7 pCEP4 and HuH7 pCEP4-GNMT cells. Restoring GNMT activity revealed 284 CpG sites (277 genes) that lost methylation (>20 %) in HuH7 cells ectopically overexpressing *GNMT* (Fig. 4a). Interestingly, most (74 %) of these genes were less methylated in healthy liver cells than in HuH7 pCEP4 cells (Fig. 4b), which suggests that lack of GNMT might have a direct role in the de novo promoter hypermethylation in HCC. In addition, some of the genes had been previously reported to be aberrantly hypermethylated in HCC (ESM Table S3), which suggest further that GNMT plays a relevant role in the establishment of aberrant promoter methylation patterns in HCC.

To validate the methylation array data, we selected two genes that had been previously found to be hypermethylated in HCC, *PYCARD* [32] and *SOCS2* [18], and another two

genes that had never been shown to be hypermethylated in cancer, *RGS16* and *SCUBE2*. Then, we determined, by bisulfite pyrosequencing, their methylation status in the HuH7 pCEP4 and pCEP4-GNMT cells. Results corroborated the methylation array data (Fig. 4c). To investigate whether GNMT-associated promoter hypermethylation occurs also in vivo, we determined the methylation status of *RGS16* and *SOCS2* in three HCCs expressing GNMT and three HCCs showing DNA hypermethylation-dependent GNMT repression. Both genes presented much lower promoter DNA methylation levels in the primary tumors expressing GNMT (Fig. 4c), which suggests that lack of GNMT plays an important role in these genes too. Taking this into account, lack of GNMT may indeed have a direct role in the establishment of aberrant promoter hypermethylation in HCC in vivo.

In order to corroborate this possibility, we carried out genome-wide promoter DNA methylation analysis in SNU354 pCEP4-GNMT cells, which showed that
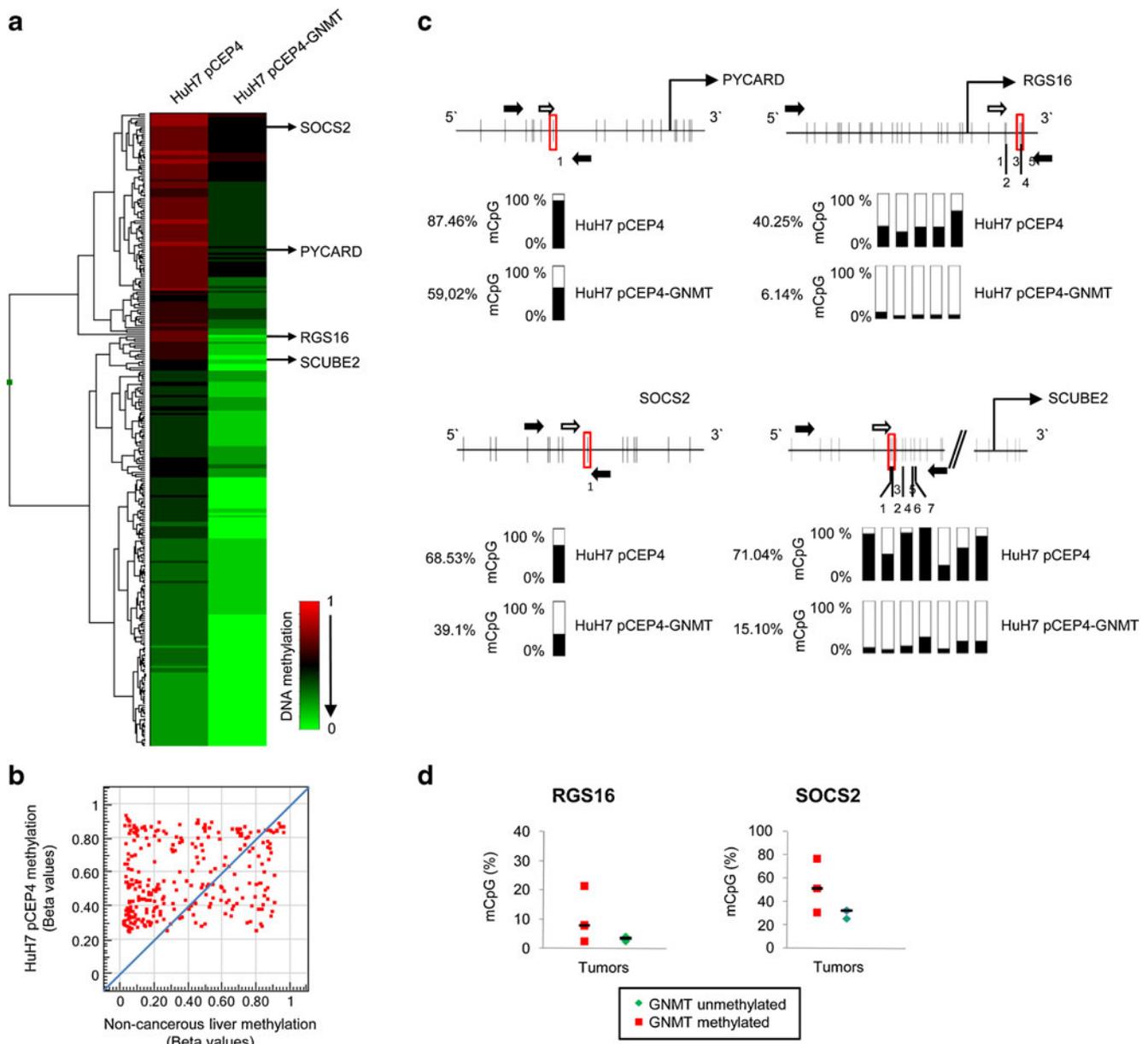
Fig. 4 Epigenetic and epigenomic consequences of GNMT restoration in HuH7 cells. **a** Clustering heat map showing the loss of DNA methylation (of at least 20 %) at the promoter region of 277 genes when GNMT is reintroduced in HuH7 cells. **b** *Scatter plot* showing differences in methylation values between HuH7-pCEP4 cells and healthy liver. **c** *Diagram bars* representing promoter methylation of candidate genes (RGS16, PYCARD, SOCS2, and SCUBE2) in HuH7 pCEP4 and HuH7 pCEP4-GNMT cells determined by bisulfite pyrosequencing. **d** Graphs representing promoter methylation of RGS16 and SOCS2 genes in three GNMT promoter hypermethylated HCC (*red*) and in another three HCC with unmethylated GNMT promoter (*green*)

restoration of GNMT was associated with the loss of methylation (>20 %) of 511 CpG sites (484 genes), most (70 %) of which were less methylated in healthy liver (ESM Fig. S7C, D). We identified 13 common probes in both transfections (bootstrap, $p < 0.01$), which suggests that there are specific regions which are more affected than others by the restoration of GNMT (ESM Table 4).

Interestingly, we also found that the loss of DNA methylation when we performed a stable transfection in both hepatic cancer cell lines (HuH7 and SNU354) was significantly more likely to occur in the promoters of those genes with enriched Polycomb occupancy (Fisher's exact test, $p < 0.001$) and the presence of bivalent histone domains (H4K4me3+H3K27me3; Fisher's exact test, $p < 0.001$) in embryonic stem cells (ESM Fig. S7E). Curiously, enrichment of these marks has been found to be associated with CpG hypermethylation in cancer [33–36].

Human data

There was no significant association between DNA methylation, GNMT mRNA expression, and the majority of the clinical parameters. Interestingly, low GNMT mRNA expression was more frequent in HCC >5 cm ($p=0.046$), in patients with increased AFP beyond 400 ng/dL ($p=0.008$) and in those with HCV-related HCC ($p=0.008$). These findings suggest a role for etiology in methylation status as well as a progressive reduction along tumor progression (Fig. 5).

Discussion

As with many other tumors, epigenetic disturbances contribute significantly to the etiology of HCC, especially DNA methylation [8]. Here, we have tried to elucidate the molecular mechanisms involved in aberrant DNA methylation in human HCC. Together with deregulation of DNA methyltransferases, abnormal regulation of the methyl group metabolism has been considered as a possible source of aberrant methylation. Thus, we focused on studying the epigenetic regulation of GNMT, a methyltransferase that catabolyzes SAMe excess and regulates total transmethylation reactions [37]. GNMT deregulation can alter methylation profiles in cells [38]. In addition, defects in GNMT are related to liver disease in humans [14, 15] and GNMT-deficient mice spontaneously develop liver steatosis and HCC [18, 26], although no mutations have been found in HCC.

Here, we show for the first time that GNMT is under abnormal epigenetic regulation in HCC. By studying the methylation status of a CpG island surrounding the TSS of GNMT in human liver cancer cell lines and HCC with

bisulfite pyrosequencing, MSP, and methylation arrays, we found that the 3′ region of the TSS of GNMT is hypermethylated to some extent. Moreover, this aberrant hypermethylation could contribute to the transcriptional silencing of the gene. AdC treatment in cell lines with high content of mC within the 3′ region of the TSS of GNMT could induce demethylation of that region and restore GNMT activity, corroborating the idea that aberrant hypermethylation may indeed be related with GNMT silencing in HCC. These results are in line with previous findings suggesting that methylation of CpG islands that spread over the 3′ region of the TSS is important for the efficient regulation of gene expression [39, 40].

GNMT expression in human HCC was dramatically lower than in healthy tissue samples. However, we found differences among unmethylated HCCs, which did not always express GNMT. This result points to DNA methylation possibly being sufficient to repress GNMT expression but that it may not be an exclusive mechanism: it may coexist with other mechanisms that can efficiently silence this gene. It seems that histone methylation could be cooperating with DNA methylation to prevent GNMT expression in cancer cells, as H3K4me3, a histone mark commonly linked to active transcriptional activity [31], was not detected in cells which lacked hypermethylation in the 3′ region but exhibited low or an absence of GNMT activity.

In the work presented here, restoration of GNMT expression dramatically reduced SAMe levels in human HCC cells. This is in line with previous findings in which GNMT deletions led to abnormally high levels of SAMe and altered methylation status in vivo depending on genetic background and environmental factors [18, 41, 42]. Our data shows that LINE1 methylation is hardly affected after restoring GNMT activity, suggesting that lack of GNMT might have different effects on genomic DNA methylation in humans and in mice. Indeed, Wang et al. [43] showed that the effect of GNMT on global methylation in human HCC cell lines was SAMe dependent [43]. In addition, GNMT expression has been shown to be modulated by SAMe itself, L-methionine and vitamin D derivatives, like transretinoic acid [38, 43]. As we have cultured cell lines in the absence of these metabolites, epigenetic and functional changes may not be as drastic as those seen in other experimental models, such as mice with systemic repression of GNMT and an exogenous supply of any of the metabolites mentioned above [18].

In contrast to LINE1, methylation arrays revealed that 277 genes lost about 20 % of methylation at the promoter region of the GNMT gene after stably transfecting GNMT in HuH7 cells. These apparently contradictory results are explained because LINE1 is distributed ubiquitously throughout the genome and therefore LINE1 methylation represents global DNA methylation [27]. As the methylation arrays analyze specific gene promoter DNA methylation,
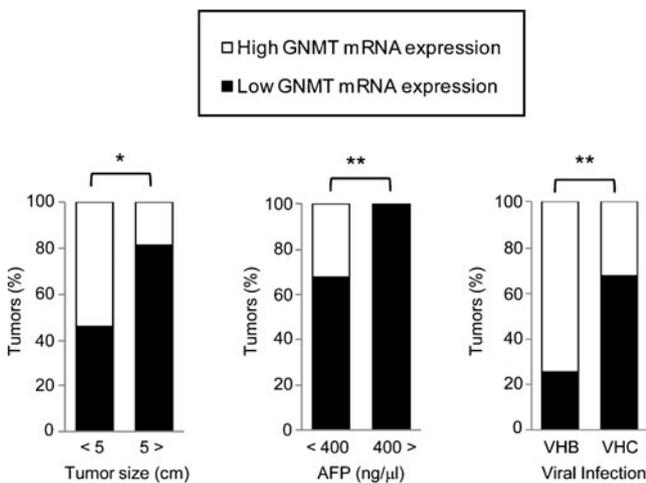
Fig. 5 Correlations between GNMT mRNA expression and several clinicopathological features. Lower levels of GNMT mRNA expression directly correlate with larger tumor size (right, p value 0.046), higher levels of AFP (middle, p value 0.006), and hepatitis C viral infection (left, p value 0.006)

which represents a small percentage of the genome, the observed hypermethylation at these sequences is compatible with the absence of global DNA methylation changes. In a similar way, recovery of GNMT activity in SNU354 cells led to the loss of promoter methylation in 484 genes. Interestingly, 13 genes of these genes were common to both cell lines which suggest that they could be more susceptible to suffering GNMT-dependent changes of DNA methylation. The different target identified in both cells lines suggests that the effect of GNMT on DNA methylation is also highly dependent on the context in which this tumor occurs.

Interestingly, most of the genes that lost methylation at the promoter region of the GNMT gene after stably transfecting GNMT were usually hypomethylated in healthy liver. Some of the genes that lost methylation in response to GNMT expression, like *PYCARD* [32] and *SOCS2* [18], have been previously reported to be aberrantly hypermethylated in HCC. For instance, loss of *SOCS2* promotes cell growth in different scenarios [44, 45]. In primary ovarian cancers, *SOCS2* is transcriptionally inactive due to aberrant promoter hypermethylation [46]. More recently, GNMT-KO mice exhibited increased SOCS2 promoter hypermethylation and developed liver steatosis and HCC [18]. In the case of PYCARD, a candidate TSG with pro-apoptotic properties has been reported to be silenced by promoter hypermethylation in many cancer types, including HCC [32].

The other two validated genes, RGS16 and SCUBE2, had not been previously associated with HCC. However, RGS16, a p53 target gene [47], has been found to be methylated and underexpressed in some breast tumors, increasing cell growth and suggesting that it could be acting as a TSG [48]. SCUBE2 has been also associated with breast cancer, and is a prognostic marker for favorable clinical outcome [49].

These results evidence a possible role for GNMT in hepatocarcinogenesis as already suggested by previous work on GNMT KO mice [18] and, more precisely, in the establishment of the HCC-specific genome-wide promoter hypermethylation signature, giving rise to a new line of research which could be focused on the aforementioned genes, which could exert an anticancer function.

HCC represents a very heterogeneous group of cancers. Both tumor background in terms of etiology or risk factors, and evolutionary events can influence the degree of epigenetic change and GNMT expression. For instance, tumor size correlated negatively with GNMT mRNA expression. According to this, in vitro assays proved that restoring GNMT induced a minor decrease in cell growth, reinforcing the hypothesis of GNMT as a TSG in hepatic cancer as proposed by previous studies [17, 18]. Elevated serum AFP levels are useful to define patients at risk for HCC and also identify HCC patients with poorer prognosis and faster progression rate [3, 50]. In this sense, tumors with high levels of AFP in serum correlate with low GNMT

expression, and this reinforces the role of GNMT expression and methylation status in HCC prognosis. Finally, the relationship between HCV infection and higher GNMT expression levels raises again the controversy of the potential etiology-based heterogeneity in tumor evolution.

In conclusion, we have shown that aberrant DNA methylation is at least in part responsible for transcriptional silencing of *GNMT* in hepatocarcinogenesis. The overexpression of this gene in HCC cells tends to suppress tumorigenicity in vitro. Histone and genome-wide methylation analyses suggest that deregulation of GNMT in HCC does not induce major changes at repeated DNA methylation but that it is more related to promoter-specific DNA methylation of TSGs.

References

1. Jemal A, Bray F, Center MM, Ferlay J, Ward E, Forman D (2011) Global cancer statistics. CA Cancer J Clin 61:69–90
2. Forner A, Llovet JM, Bruix J (2012) Hepatocellular carcinoma. Lancet 379:1245–1255
3. Bruix J, Sherman M (2011) Management of hepatocellular carcinoma: an update. Hepatology 53:1020–1022
4. Marrero JA, Fontana RJ, Fu S, Conjeevaram HS, Su GL, Lok AS (2005) Alcohol, tobacco and obesity are synergistic risk factors for hepatocellular carcinoma. J Hepatol 42:218–224
5. Fracanzani AL, Conte D, Fraquelli M, Taioli E, Mattioli M, Losco A, Fargion S (2001) Increased cancer risk in a cohort of 230 patients with hereditary hemochromatosis in comparison to matched control patients with non-iron-related chronic liver disease. Hepatology 33:647–651
6. El-Serag HB, Hampel H, Javadi F (2006) The association between diabetes and hepatocellular carcinoma: a systematic review of epidemiologic evidence. Clin Gastroenterol Hepatol 4:369–380
7. Bugianesi E, Leone N, Vanni E, Marchesini G, Brunello F, Carucci P, Musso A, De Paolis P, Capussotti L, Salizzoni M et al (2002) Expanding the natural history of nonalcoholic steatohepatitis:

from cryptogenic cirrhosis to hepatocellular carcinoma. Gastroenterology 123:134–140

8. Thorgeirsson SS, Grisham JW (2002) Molecular pathogenesis of human hepatocellular carcinoma. Nat Genet 31:339–346

9. Kanai Y, Ushijima S, Hui AM, Ochiai A, Tsuda H, Sakamoto M, Hirohashi S (1997) The E-cadherin gene is silenced by CpG methylation in human hepatocellular carcinomas. Int J Cancer 71:355–359

10. Ito T, Nishida N, Fukuda Y, Nishimura T, Komeda T, Nakao K (2004) Alteration of the p14(ARF) gene and p53 status in human hepatocellular carcinomas. J Gastroenterol 39:355–361

11. Wong IH, Lo YM, Zhang J, Liew CT, Ng MH, Wong N, Lai PB, Lau WY, Hjelm NM, Johnson PJ (1999) Detection of aberrant p16 methylation in the plasma and serum of liver cancer patients. Cancer Res 59:71–73

12. Kerr SJ (1972) Competing methyltransferase systems. J Biol Chem 247:4248–4252

13. Uthus EO, Ross SA, Davis CD (2006) Differential effects of dietary selenium (se) and folate on methyl metabolism in liver and colon of rats. Biol Trace Elem Res 109:201–214

14. Augoustides-Savvopoulou P, Luka Z, Karyda S, Stabler SP, Allen RH, Patsiaoura K, Wagner C, Mudd SH (2003) Glycine N-methyltransferase deficiency: a new patient with a novel mutation. J Inherit Metab Dis 26:745–759

15. Mudd SH, Cerone R, Schiaffino MC, Fantasia AR, Minniti G, Caruso U, Lorini R, Watkins D, Matiaszuk N, Rosenblatt DS et al (2001) Glycine N-methyltransferase deficiency: a novel inborn error causing persistent isolated hypermethioninaemia. J Inherit Metab Dis 24:448–464

16. Chen YM, Shiu JY, Tzeng SJ, Shih LS, Chen YJ, Lui WY, Chen PH (1998) Characterization of glycine-N-methyltransferase-gene expression in human hepatocellular carcinoma. Int J Cancer 75:787–793

17. Liu HH, Chen KH, Shih YP, Lui WY, Wong FH, Chen YM (2003) Characterization of reduced expression of glycine N-methyltransferase in cancerous hepatic tissues using two newly developed monoclonal antibodies. J Biomed Sci 10:87–97

18. Martinez-Chantar ML, Vazquez-Chantada M, Ariz U, Martinez N, Varela M, Luka Z, Capdevila A, Rodriguez J, Aransay AM, Matthiesen R et al (2008) Loss of the glycine N-methyl transferase gene leads to steatosis and hepatocellular carcinoma in mice. Hepatology 47:1191–1199

19. Farber E, Ichinose H (1958) The prevention of ethionine-induced carcinoma of the liver in rats by methionine. Cancer Res 18:1209–1213

20. Pascale RM, Marras V, Simile MM, Daino L, Pinna G, Bennati S, Carta M, Seddaiu MA, Massarelli G, Feo F (1992) Chemoprevention of rat liver carcinogenesis by S-adenosyl-L-methionine: a long-term study. Cancer Res 52:4979–4986

21. Shivapurkar N, Hoover KL, Poirier LA (1986) Effect of methionine and choline on liver tumor promotion by phenobarbital and DDT in diethylnitrosamine-initiated rats. Carcinogenesis 7:547–550

22. Balaghi M, Horne DW, Wagner C (1993) Hepatic one-carbon metabolism in early folate deficiency in rats. Biochem J 291(Pt 1):145–149

23. Ogawa H, Gomi T, Takusagawa F, Fujioka M (1998) Structure, function and physiological role of glycine N-methyltransferase. Int J Biochem Cell Biol 30:13–26

24. Wagner C, Briggs WT, Cook RJ (1985) Inhibition of glycine N-methyltransferase activity by folate derivatives: implications for regulation of methyl group metabolism. Biochem Biophys Res Commun 127:746–752

25. Pascale RM, Simile MM, De Miglio MR, Nufris A, Daino L, Seddaiu MA, Rao PM, Rajalakshmi S, Sarma DS, Feo F (1995) Chemoprevention by S-adenosyl-L-methionine of rat liver carcinogenesis initiated by 1,2-dimethylhydrazine and promoted by orotic acid. Carcinogenesis 16:427–430

26. Liao YJ, Liu SP, Lee CM, Yen CH, Chuang PC, Chen CY, Tsai TF, Huang SF, Lee YH, Chen YM (2009) Characterization of a glycine N-methyltransferase gene knockout mouse model for hepatocellular carcinoma: implications of the gender disparity in liver cancer susceptibility. Int J Cancer 124:816–826

27. Yang AS, Estecio MR, Doshi K, Kondo Y, Tajara EH, Issa JP (2004) A simple method for estimating global DNA methylation using bisulfite PCR of repetitive DNA elements. Nucleic Acids Res 32:e38

28. Livak KJ, Schmittgen TD (2001) Analysis of relative gene expression data using real-time quantitative PCR and the 2(-delta delta C (T)) method. Methods 25:402–408

29. Mosmann T (1983) Rapid colorimetric assay for cellular growth and survival: application to proliferation and cytotoxicity assays. J Immunol Methods 65:55–63

30. Shechter D, Dormann HL, Allis CD, Hake SB (2007) Extraction, purification and analysis of histones. Nat Protoc 2:1445–1457

31. Ruthenburg AJ, Allis CD, Wysocka J (2007) Methylation of lysine 4 on histone H3: intricacy of writing and reading a single epigenetic mark. Mol Cell 25:15–30

32. Zhang C, Li H, Zhou G, Zhang Q, Zhang T, Li J, Zhang J, Hou J, Liew CT, Yin D (2007) Transcriptional silencing of the TMS1/ASC tumour suppressor gene by an epigenetic mechanism in hepatocellular carcinoma cells. J Pathol 212:134–142

33. Fernandez AF, Assenov Y, Martin-Subero JI, Balint B, Siebert R, Taniguchi H, Yamamoto H, Hidalgo M, Tan AC, Galm O et al (2012) A DNA methylation fingerprint of 1628 human samples. Genome Res 22:407–419

34. Ohm JE, McGarvey KM, Yu X, Cheng L, Schuebel KE, Cope L, Mohammad HP, Chen W, Daniel VC, Yu W et al (2007) A stem cell-like chromatin pattern may predispose tumor suppressor genes to DNA hypermethylation and heritable silencing. Nat Genet 39:237–242

35. Schlesinger Y, Straussman R, Keshet I, Farkash S, Hecht M, Zimmerman J, Eden E, Yakhini Z, Ben-Shushan E, Reubinoff BE et al (2007) Polycomb-mediated methylation on Lys27 of histone H3 pre-marks genes for de novo methylation in cancer. Nat Genet 39:232–236

36. Widschwendter M, Fiegl H, Egle D, Mueller-Holzner E, Spizzo G, Marth C, Weisenberger DJ, Campan M, Young J, Jacobs I et al (2007) Epigenetic stem cell signature in cancer. Nat Genet 39:157–158

37. Mudd SH, Brosnan JT, Brosnan ME, Jacobs RL, Stabler SP, Allen RH, Vance DE, Wagner C (2007) Methyl balance and transmethylation fluxes in humans. Am J Clin Nutr 85:19–25

38. Rowling MJ, McMullen MH, Schalinske KL (2002) Vitamin A and its derivatives induce hepatic glycine N-methyltransferase and hypomethylation of DNA in rats. J Nutr 132:365–369

39. Appanah R, Dickerson DR, Goyal P, Groudine M, Lorincz MC (2007) An unmethylated 3′ promoter-proximal region is required for efficient transcription initiation. PLoS Genet 3:e27

40. Deaton AM, Webb S, Kerr AR, Illingworth RS, Guy J, Andrews R, Bird A (2011) Cell type-specific DNA methylation at intragenic CpG islands in the immune system. Genome Res 21:1074–1086

41. Liu SP, Li YS, Chen YJ, Chiang EP, Li AF, Lee YH, Tsai TF, Hsiao M, Huang SF, Chen YM (2007) Glycine N-methyltransferase⁻/⁻ mice develop chronic hepatitis and glycogen storage disease in the liver. Hepatology 46:1413–1425

42. Luka Z, Capdevila A, Mato JM, Wagner C (2006) A glycine N-methyltransferase knockout mouse model for humans with deficiency of this enzyme. Transgenic Res 15:393–397

43. Wang YC, Tang FY, Chen SY, Chen YM, Chiang EP (2011) Glycine-N methyltransferase expression in HepG2 cells is involved in methyl group homeostasis by regulating transmethylation kinetics and DNA methylation. J Nutr 141:777–782

44. Metcalf D, Greenhalgh CJ, Viney E, Willson TA, Starr R, Nicola NA, Hilton DJ, Alexander WS (2000) Gigantism in mice lacking suppressor of cytokine signalling-2. Nature 405:1069–1073

45. Schultheis B, Carapeti-Marootian M, Hochhaus A, Weisser A, Goldman JM, Melo JV (2002) Overexpression of SOCS-2 in advanced stages of chronic myeloid leukemia: possible inadequacy of a negative feedback mechanism. Blood 99:1766–1775

46. Sutherland KD, Lindeman GJ, Choong DY, Wittlin S, Brentzell L, Phillips W, Campbell IG, Visvader JE (2004) Differential hypermethylation of SOCS genes in ovarian and breast carcinomas. Oncogene 23:7726–7733

47. Buckbinder L, Velasco-Miguel S, Chen Y, Xu N, Talbott R, Gelbert L, Gao J, Seizinger BR, Gutkind JS, Kley N (1997) The p53 tumor suppressor targets a novel regulator of G protein signaling. Proc Natl Acad Sci U S A 94:7868–7872

48. Liang G, Bansal G, Xie Z, Druey KM (2009) RGS16 inhibits breast cancer cell growth by mitigating phosphatidylinositol 3-kinase signaling. J Biol Chem 284:21719–21727

49. Cheng CJ, Lin YC, Tsai MT, Chen CS, Hsieh MC, Chen CL, Yang RB (2009) SCUBE2 suppresses breast tumor cell proliferation and confers a favorable prognosis in invasive breast cancer. Cancer Res 69:3634–3641

50. Sherman M (2010) The resurrection of alphafetoprotein. J Hepatol 52:939–940